Journal of Alloys and Compounds 680 (2016) 617–622

Contents lists available at ScienceDirect

Journal of Alloys and Compounds

journal homepage: http://www.elsevier.com/locate/jalcom

Large magnetocaloric effect in $Er_{12}Co_7$ compound and the enhancement of δT_{FWHM} by Ho-substitution

Xinqi Zheng [a], Bo Zhang [b], Yueqiao Li [b], Hui Wu [c], Hu Zhang [a], Jingyan Zhang [a], Shouguo Wang [a, *], Qingzhen Huang [c], Baogen Shen [b]

[a] School of Materials Science and Engineering, University of Science and Technology Beijing, Beijing, 100083, PR China
[b] State Key Laboratory for Magnetism, Institute of Physics, Chinese Academy of Sciences, Beijing, 100190, PR China
[c] NIST Center for Neutron Research, National Institute of Standards and Technology, Gaithersburg, MD, 20899, USA

ARTICLE INFO

Article history:
Received 31 January 2016
Received in revised form
19 April 2016
Accepted 21 April 2016
Available online 21 April 2016

Keywords:
Magnetocaloric effect
$RE_{12}Co_7$ compound
Magnetic refrigerant materials

ABSTRACT

Polycrystalline monoclinic $Er_{12}Co_7$ compound with a large magnetocaloric effect (MCE) was synthesized. The maximum values of the magnetic entropy change (ΔS_M) under the field changes of 0–2 T and 0–5 T reach 10.2 J/kgK and 18.3 J/kgK, respectively. In order to gain further insight in understanding the MCE, samples with various Ho substitutions for Er were fabricated and studied. It was found that Ho-substitution makes a great impact on the magnetic properties and MCE of $Er_{12}Co_7$ compound. Through compositional optimization, the mixed product of $Ho_{12}Co_7$ and $Er_6Ho_6Co_7$ with the weight ratio of 58:42 was tailored to exhibit the best MCE performance. The maximum value of ΔS_M, the full width at half maximum of ΔS_M-T curve and the refrigerant capacity of the mixed compound are calculated to be 16.7 J/kgK, 37.9 K and 522 J/kg, respectively.

1. Introduction

Magnetocaloric effect (MCE) is one of the instinct properties of magnetic materials, and the magnetic refrigeration based on MCE has been demonstrated as a promising alternative to the conventional gas compression/expansion refrigeration due to its environmental friendliness and high efficiency [1–4]. A lot of efforts have been devoted to explore room temperature MCE materials for applications in household refrigerators or air conditioners. The typical room temperature MCE materials mainly include $Gd_5Si_2Ge_2$, $La(Fe,Si)_{13}$, $MnAs_{1-x}Sb_x$, $MnFeP_{1-x}As_x$, NiMnGa and NiMnIn [4–17]. Recently, MCE materials used for gas liquefaction at low temperature have drawn much attention. The reported low temperature MCE materials mainly include the rare earth (RE) based compounds, such as REAgAl (RE = Ho, Er), DyNiSi, ErRuSi, $TbCo_3B_2$, CeSi, Ho(Ni,Cu)Al [18–23] etc. MCE materials are generally evaluated by the following parameters: the maximum value of magnetic entropy change $(-(\Delta S_M)_{max})$, the full width at half maximum of ΔS_M-T curve (δT_{FWHM}), refrigerant capacity (RC) and adiabatic temperature change (ΔT_{ad}). The materials with multi-transitions show some advantages on broadening of δT_{FWHM}, such as ErGa and HoZn [24,25]. Furthermore, a table-like plateau is observed on the ΔS_M-T curve of PrGa and $GdCd_{0.9}Ru_{0.1}$ compounds [26–28]. This type of plateau is significantly valuable for practical applications, and much efforts have been devoted to design new compounds exhibiting such table-like ΔS_M-T curves such as REFeSi (RE = Tb, Dy) [29].

The RE-Co series belong to the category of the RE-based compounds, and lots of RE-Co-based compounds have been investigated on their magnetic properties and MCE [30–32]. $RE_{12}Co_7$ (RE = Gd, Tb, Dy, Ho, Er) polycrystalline samples possess monoclinic structures (space group $P2_1/c$ #14) [33] with four different types of Co-centered RE polyhedra in the unit cell: trigonal prism, cube, Archimedian antiprism and truncated Archimedian antiprism [33]. The magnetic properties of $Gd_{12}Co_7$, $Tb_{12}Co_7$, $Gd_4Tb_8Co_7$, $Gd_8Tb_4Co_7$ and $Dy_{12}Co_7$ have been studied and they were found to undergo only one ferromagnetic (FM) to paramagnetic (PM) transition [34–37]. For $Gd_{12}Co_7$, a spin reorientation transition was reported at 123 K [37]. More recently, $Ho_{12}Co_7$ compound has been found to undergo three transitions including from AFM to AFM, from AFM to FM and from FM to PM at 9 K, 17 K and 30 K, respectively [38]. According to the previous work, Co atoms were found to slightly contribute to the magnetic moments in $Ho_{12}Co_7$ [38] and $Dy_{12}Co_7$ [36] compounds. The magnetocaloric effect for most of the $RE_{12}Co_7$ compounds has been studied, but the MCE

* Corresponding author.
E-mail address: sgwang@ustb.edu.cn (S. Wang).

http://dx.doi.org/10.1016/j.jallcom.2016.04.216
0925-8388/

behavior of $Er_{12}Co_7$ has not been investigated.

In this paper, polycrystalline $Er_{12}Co_7$ compound was synthesized and large MCE was observed. In order to tune the MCE, Ho was used to substitute Er with different concentrations (x = 0, 4, 6, 8, 10, 12) in $Er_{12-x}Ho_xCo_7$ compounds. In order to obtain the table-like ΔS_M-T curves, $Er_{12-x}Ho_xCo_7$ compounds with different compositions were mixed and the mixing ratio was optimized. The effect of the total angular momentum quantum number and the spin exchange coupling on the MCE of Ho-doped $Er_{12-x}Ho_xCo_7$ compounds is analyzed and discussed.

2. Experimental

Polycrystalline $Er_{12-x}Ho_xCo_7$ (x = 0, 4, 6, 8, 10, 12) compounds were prepared by arc-melting method in a high-purity argon atmosphere. The purities of starting materials were better than 99.9%. The ingots were turned over and remelted several times to ensure their homogeneity. After arc-melting, the samples were subsequently wrapped with molybdenum foils, sealed in a high-vacuum quartz tube, annealed at 750 °C for 7 days and finally quenched in liquid nitrogen. Crystal structures were characterized by powder X-ray diffraction (XRD) method with Cu Kα radiation. Magnetic measurements (including M-T and M-H curves) were carried out by employing Vibrating Sample Magnetometer with Quantum Design (SQUID-VSM). The data of $Ho_{12}Co_7$ compound were cited from our previous work [38].

3. Results and discussion

The powder XRD measurements of $Er_{12}Co_7$ and Ho-doped $Er_{12-x}Ho_xCo_7$ (x = 4, 6, 8, 10, 12) compounds were carried out at room temperature. Fig. 1 shows the XRD pattern and Rietveld refinement analysis of $Er_{12}Co_7$ and its crystal structure. All diffraction peaks can be well indexed to a monoclinic crystal structure (space group $P2_1/c$ #14). The goodness of refinement factors are $\chi^2 = 1.926$, $wR_p = 5.48\%$ and $R_p = 4.34\%$, respectively. The lattice parameters are determined as a = 8.2743(5) Å, b = 11.0857(1) Å, c = 13.7351(2) Å and β = 138.8°. In one unit cell, 24 Er atoms and 14 Co atoms occupy six and four crystallographically distinct atomic positions, respectively, in good agreement with the reported results [33]. The XRD (not shown here) patterns collected on the Ho-doped $Er_{12-x}Ho_xCo_7$ (x = 4, 6, 8, 10, 12) compounds confirm the formation of single phases with the same crystal structure as that of $Er_{12}Co_7$ compound.

The zero-field-cooled (ZFC) and field-cooled (FC) magnetization curves for $Er_{12}Co_7$ and Ho-doped $Er_{12-x}Ho_xCo_7$ (x = 4, 6, 8, 10, 12) compounds were measured under a field of 0.01 T. The ZFC and FC curves for $Er_{12}Co_7$ compound were shown in Fig. 2(a). The magnetization of $Er_{12}Co_7$ compound shows a clear increase and then a decrease with increasing temperature. Two drastic changes were observed at $T_t = 6.5$ K and $T_C = 13.5$ K, corresponding to the transitions from AFM to FM and from FM to PM, respectively. The detailed analysis about the magnetic transitions will be discussed in the next section. The overlap of ZFC and FC curves around T_C indicates its good thermal reversibility in $Er_{12}Co_7$ compound. The non-coincidence of ZFC and FC curves at lower temperature may result from the domain-wall pinning effect [24]. Inset of Fig. 2(a) shows the temperature dependence of χ^{-1} in PM zone and the fitting curve, where χ is the magnetic susceptibility. A linear fitting can be clearly observed, and the effective moment (M_{eff}) of Er atom was calculated to be 10.1 μ_B, which is a little larger than that of the free Er^{3+} ion (9.6 μ_B). In the previous works, Co atoms were considered to be non-magnetic because the 3d bands are filled by 6s and 5d electrons of the Tb atoms in $Tb_{12}Co_7$ compound [34,39]. Another viewpoint is also applied where Co atoms are considered to have a small contribution to the magnetic moment in $Ho_{12}Co_7$ and $Dy_{12}Co_7$ compounds [36,38]. However, no direct evidence has been provided to prove the magnetic contribution of Co atoms in $RE_{12}Co_7$ compounds. Therefore, for the $Er_{12-x}Ho_xCo_7$ series

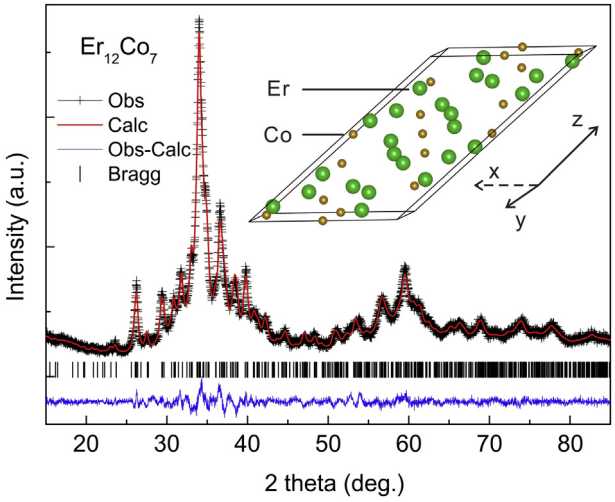

Fig. 1. The XRD pattern and Rietveld refinement fitting curve for $Er_{12}Co_7$ compound at 295 K. The experimental data and the calculated patterns are plotted in cross and solid line, respectively. The solid line at the bottom is the difference between the experimental and calculated profiles. The Bragg positions are marked as short vertical lines. Inset: the crystal structure of $Er_{12}Co_7$ compound in one unit cell.

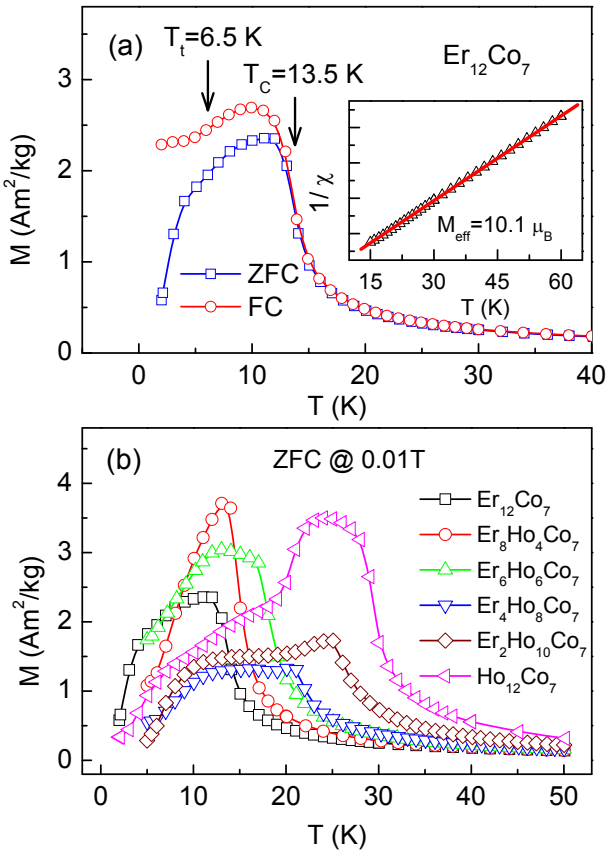

Fig. 2. (a) ZFC and FC curves of $Er_{12}Co_7$ compound at a field of 0.01 T. Inset: temperature dependence curve of χ^{-1} and the fitting, where χ is the magnetic susceptibility. (b) ZFC curves for $Er_{12-x}Ho_xCo_7$ (x = 0, 4, 6, 8, 10, 12) compounds at a field of 0.01 T.

investigated here, it is reasonable to conclude that the contribution of Co on magnetic moments is negligible and rare earth atoms play a dominant role in the magnetic moments. The ZFC curves for $Er_{12-x}Ho_xCo_7$ (x = 0, 4, 6, 8, 10, 12) compounds were shown in Fig. 2(b). $Er_{12}Co_7$ and the lower doping (x = 4, 6, and 8) compounds exhibit different transition behaviors, compared to the samples with higher doping levels (x = 10 and 12). For samples with lower doping, two drastic changes of M-T curves were observed, corresponding to two magnetic transitions as same as observed in $Er_{12}Co_7$ compound, i.e., $Er_{12-x}Ho_xCo_7$ (x = 0, 4, 6, 8) compounds undergo an AFM to FM transition at T_t and an FM to PM transition at T_C with increasing temperature. The values of T_t for $Er_{12-x}Ho_xCo_7$ (x = 0, 4, 6, 8) compounds are 6.5 K, 8.6 K, 12.0 K and 11.0 K, respectively. The values of T_C for $Er_{12-x}Ho_xCo_7$ (x = 0, 4, 6, 8) compounds are 13.5 K, 15.0 K, 18.0 K and 22.0 K, respectively. For samples with higher doping (x = 10 and 12), three magnetic transitions were observed. With increasing temperature, the compounds undergo an AFM to AFM transition, an AFM to FM transition and an FM to PM transition in sequence. The transition temperatures of $Er_2Ho_{10}Co_7$ compound are 9.0 K, 19.0 K and 26.3 K, respectively. For $Ho_{12}Co_7$ compound, the transition temperatures are 9 K, 17 K and 30 K, respectively [38].

Detailed isothermal magnetization (M-H) curves up to 7 T were also measured for $Er_{12}Co_7$ compound at the temperatures from 3 K to 47 K as shown in Fig. 3(a). Enlarged M-H curves at low fields at 5 K, 6 K and 7 K were provided in Fig. 3(b). When the magnetic field is lower than 0.36 T, M at 7 K shows the largest value while M at 5 K is the smallest. When magnetic fields are higher than 0.36 T, the rank of magnetization value is in a reverse order with larger M (5 K/6 K) and smaller M (7 K). It indicates that the magnetic ground state of $Er_{12}Co_7$ compound at low temperature is weak AFM. A similar analysis method was also reported previously [38]. The system shows typical FM characteristics in the temperature range between 7.0 K and 13 K and PM behavior above 13 K. Therefore, as temperature increases, two magnetic transitions from AFM to FM and from FM to PM are confirmed for $Er_{12}Co_7$ compound. The Arrott plots of $Er_{12}Co_7$ compound can be obtained from the M-H data as shown in Fig. 3(c). The second-order phase transition property was confirmed in $Er_{12}Co_7$ compound based on the positive slope of the curves [40]. This property is in accord with the good thermal reversibility mentioned before, because it has been proven that thermal hysteresis and magnetic hysteresis are rather small for the magnetic materials with second-order phase transition [24]. Furthermore, the second-order phase transition property around T_t indicates that the transition from AFM to FM is a pure magnetic transition without volume/symmetry change, because the magneto-structural transition is usually accompanied by first-order transition in most cases [41].

Similar analysis method was performed for other Ho-doped $Er_{12-x}Ho_xCo_7$ compounds as well. Fig. 3(d) shows the M-H curves of $Er_2Ho_{10}Co_7$ compound at low fields at 5 K, 9 K and 13 K, respectively. For low field around 0.3 T, the magnetization of $Er_2Ho_{10}Co_7$ compound increases with increasing temperature from 5 K to 13 K (see inset of Fig. 3(d)). However, the magnetization

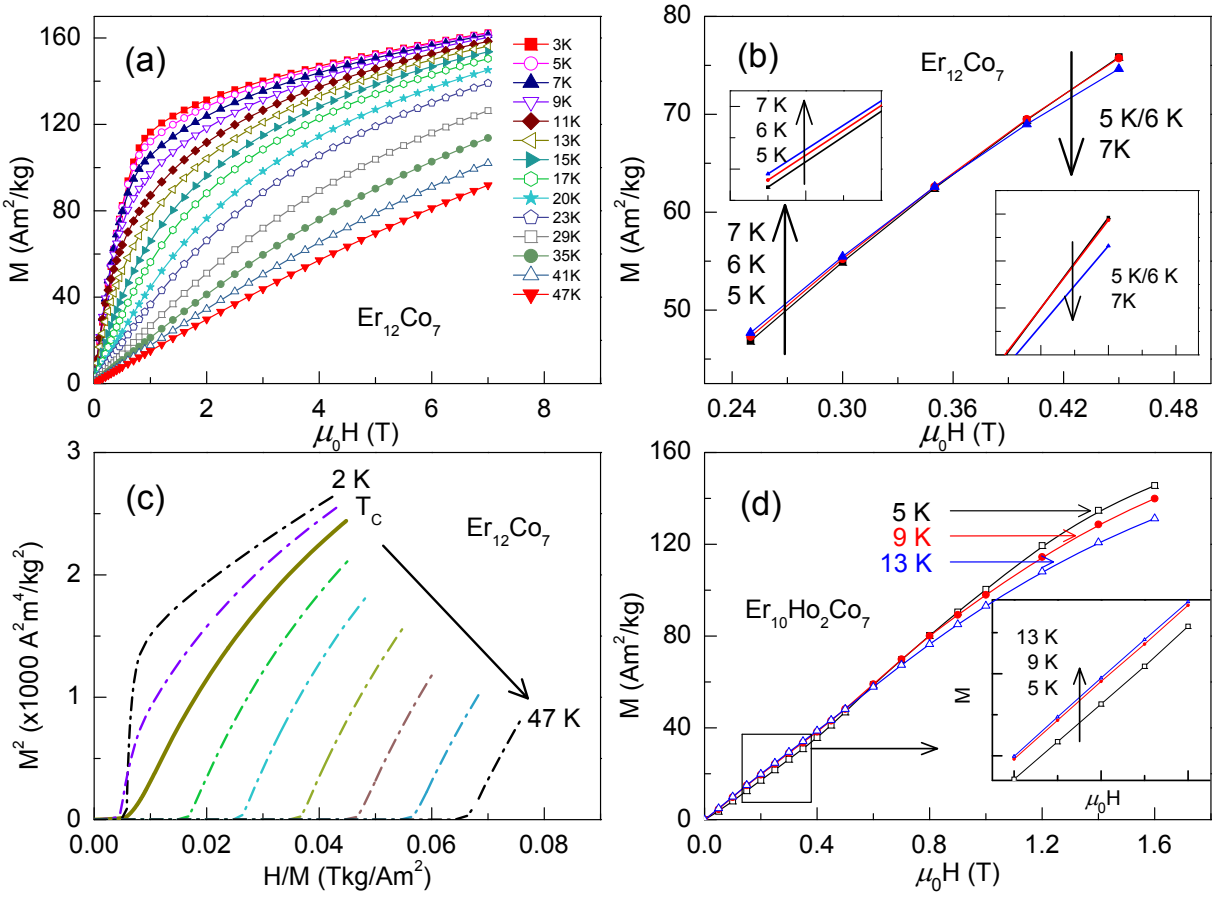

Fig. 3. (a) Field dependence of magnetization curves of $Er_{12}Co_7$ compound up to 7 T at the temperatures from 3 K to 47 K. (b) M-H curves of $Er_{12}Co_7$ compound at low fields at 5 K, 6 K and 7 K, respectively. (c) The Arrott plots of $Er_{12}Co_7$ compound at temperatures from 3 K to 47 K. (d) M-H curves of $Er_{12-x}Ho_xCo_7$ compound at low fields at 5 K, 9 K and 13 K, respectively.

shows an inverse trend at higher fields, such as 1 T. Above results indicate that the ground state is AFM below 9 K for $Er_2Ho_{10}Co_7$ compound. Besides, the AFM ground state is so weak that it can be destroyed by small magnetic fields. Furthermore, the ground state is AFM between 9 K and 19 K, FM between 19 K and 26 K, and PM above 26 K, respectively, which confirms that $Er_2Ho_{10}Co_7$ compound undergoes an AFM to AFM transition, an AFM to FM transition and an FM to PM transition in sequence. The transition property of $Er_2Ho_{10}Co_7$ compound is similar to that of $Ho_{12}Co_7$ compound [38]. Spin reorientation behavior observed in $Gd_{12}Co_7$ compound was previously ascribed to the competition between magnetic exchange and crystalline electric field [37,42]. For the present $Er_2Ho_{10}Co_7$ and $Ho_{12}Co_7$ compound, there are different types of AFM orders at low temperature, which are related to the crystalline electric fields. Therefore it is reasonable to deduce that the transition from AFM to AFM around 9 K may result from the competition between the two different AFM orders.

The magnetic transitions of Ho-doped $Er_{12-x}Ho_xCo_7$ (x = 0, 4, 6, 8, 10, 12) compounds were analyzed in detail, and the transition temperatures are listed in Table 1. It can be seen that Ho substitution has an obvious influence on the magnetic transition type and transition temperature. With increasing Ho content, the number of transitions increases from two to three. The transition at T_t is affected by the competition of two ordered magnetic states. According to Table 1, the value of T_t does not show much variation (less than 5.5 K) with increasing Ho content. This tiny variation comes from the small influence of Ho-doping on the crystal structure and crystalline electric field. The similar results were found for spin reorientation transition temperature in $Er_xHo_{1-x}Al_2$ compounds [43]. It is of great interest to find that the Curie temperature increases steadily with increasing Ho-doping. As it is analyzed before, rare earth atoms play a dominant role in the magnetic moments in $Er_{12-x}Ho_xCo_7$ compounds. Therefore, the RE-RE magnetic exchange interaction is the main magnetic coupling and the Curie temperature mainly depends on the spin-spin exchange interaction, i.e., Curie temperature is positively correlated with S (spin angular quantum number) for $Er_{12-x}Ho_xCo_7$ compounds. Since more Ho atoms induces larger averaged S for the compounds, Curie temperature increases monotonously as the content of Ho increases.

The magnetic entropy change (ΔS_M) is calculated from isothermal magnetization data (M-H curves) by using Maxwell relation $\Delta S_M(T) = -\int_0^B (\partial M/\partial T)dB$. Fig. 4(a) and Fig. 4(b) shows the ΔS_M-T curves of $Er_{12-x}Ho_xCo_7$ (x = 0, 4, 6, 8, 10, 12) compounds for the field changes of 0–2 T and 0–5 T, respectively. The maximum values of ΔS_M ($(\Delta S_M)_{max}$) for $Er_{12}Co_7$ compound are 10.2 J/kgK and 18.3 J/kgK for the field changes of 0–2 T and 0–5 T, respectively.

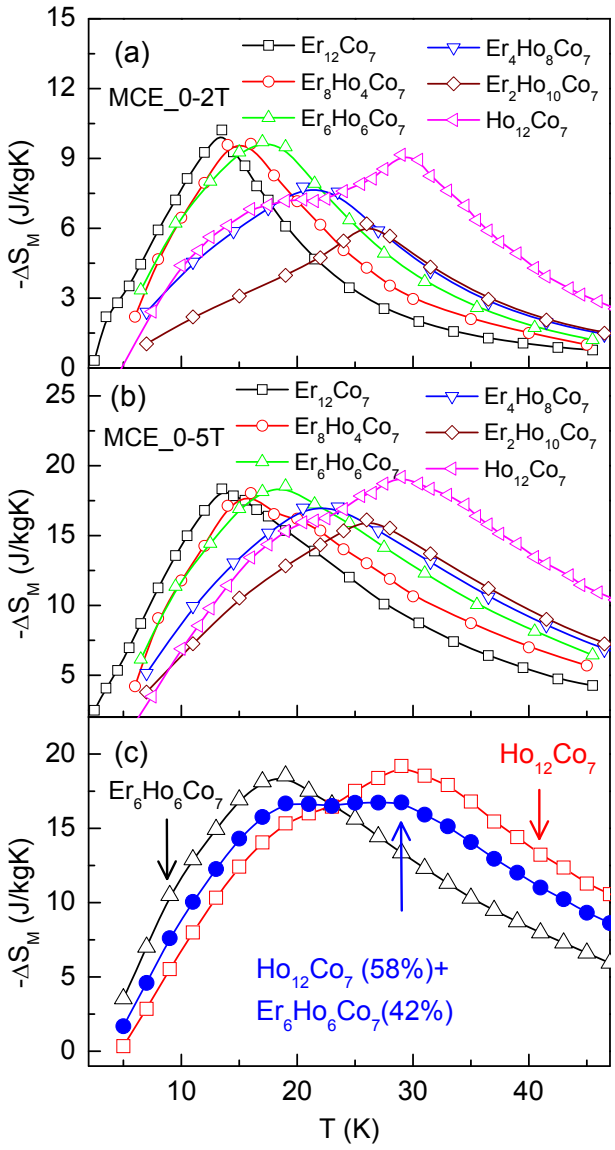

Fig. 4. (a) Temperature dependence of ΔS_M under a field change of 0–2 T for $Er_{12-x}Ho_xCo_7$ (x = 0, 4, 6, 8, 10, 12) compounds, respectively. (b) Temperature dependence of ΔS_M under a field change of 0–5 T. (c) ΔS_M of $Er_{12-x}Ho_xCo_7$ (x = 6, 12) compounds and the mixed compounds at a weight ratio of 42:58 under a field change of 0–5 T.

Table 1
The transition temperatures and magnetocaloric parameters of $RE1_{12-x}RE2_xCo_7$ (RE1,RE2 = Gd, Tb, Dy, Ho, Er; x = 0, 4, 6, 8, 10, 12) compounds.

Materials	T_t (K)	T_C (K)	MCE_0–2T			MCE_0–5T			Refs.
			$-\Delta S_M(T)_{max}$ (J/kgK)	δT_{FWHM} (K)	RC (J/kg)	$-\Delta S_M(T)_{max}$ (J/kgK)	δT_{FWHM} (K)	RC (J/kg)	
$Er_{12}Co_7$	6.5	13.5	10.2	14.5	103.6	18.3	22.8	317	This work
$Er_8Ho_4Co_7$	8.6	15.0	9.6	16.5	122.6	18.0	24.7	342	This work
$Er_6Ho_6Co_7$	12.0	18.0	9.7	19.7	150.5	18.6	28.5	411	This work
$Er_4Ho_8Co_7$	11.0	22.0	7.8	22.8	137.8	17.0	31.8	422	This work
$Er_2Ho_{10}Co_7$	9.0/19.0	26.3	6.2	20.9	94.8	16.1	32.5	396	This work
$Ho_{12}Co_7$	9.0/17.0	30.0	9.2	29.4	206.2	19.2	37.4	555	[38]
$Er_6Ho_6Co_7$ 42% $Ho_{12}Co_7$ (58%)	–	–	–	–	–	16.7	38.0	553	This work
$Dy_{12}Co_7$	–	64.0	5.0	21.7	81.5	10.0	42.1	304	[36]
$Tb_{12}Co_7$	–	100.0	3.1	8.7	20.5	–	–	–	[34]
$Gd_4Tb_8Co_7$	–	118.9	–	–	–	7.1	38.5	202	[37]
$Gd_8Tb_4Co_7$	–	140.8	–	–	–	8.2	51.8	316	[37]
$Gd_{12}Co_7$	123.0	163.0	4.6	37.4	123.3	8.8	71.7	463	[35,37]

Only one peak around T_C was observed in $Er_{12}Co_7$ compound, which is different from the MCE materials where two or more peaks can be observed with several transition temperatures such as ErGa compound [24]. This is because the magnetic transition at low temperature is very weak for $Er_{12}Co_7$ compound. The values of $(\Delta S_M)_{max}$ for $Er_{12-x}Ho_xCo_7$ (x = 0, 4, 6, 8, 10, 12) compounds along with other $RE_{12}Co_7$ compounds are listed in Table 1. It is worth noting the values of $(\Delta S_M)_{max}$ under a field change of 0–2 T because a field of 2 T is close to the practical operational field. $Er_{12}Co_7$ compound shows the largest $(\Delta S_M)_{max}$ among $Er_{12-x}Ho_xCo_7$ (x = 0, 4, 6, 8, 10, 12) compounds under a field change of 0–2 T. In addition, the ΔS_M shows a positive value under a field change of 0–0.5 T for $Er_{12}Co_7$ compound below T_t (not shown here), which confirms that a weak AFM state exists at low temperature for $Er_{12}Co_7$ compound. The correlation between the positive ΔS_M and AFM ground states has been discussed for other materials [44].

In addition the Ho substitution has a great impact on the shape of ΔS_M-T curve and value of $(\Delta S_M)_{max}$. The main ΔS_M peak moves towards higher temperature as the content of Ho increases because the peak position is associated with T_C. Another important result is that the shape of ΔS_M-T curve changes from a simple single-peak ($Er_{12}Co_7$, $Er_8Ho_4Co_7$, $Er_6Ho_6Co_7$) to single-peak complicated by a convex ($Er_4Ho_8Co_7$) or a long tail ($Er_2Ho_{10}Co_7$) at low temperature, and finally to double peaks for $Ho_{12}Co_7$ compound. This is because with increasing Ho-doping, the transition at low temperature becomes more obvious, and in the meanwhile more transitions emerge. It is also found that the $(\Delta S_M)_{max}$ value does not change monotonously with Ho-substitution. According to the model by Oesterreicher et al. [45], $(\Delta S_M)_{max}$ is negatively correlated with T_C and positively correlated with total angular momentum quantum number (J). From the above discussions on the relationship between T_C and S, they are positively correlated in $Er_{12-x}Ho_xCo_7$ compounds. For $Er_{12}Co_7$ compound, Ho-substitution results in the increasing of S and J simultaneously. As a result, the $(\Delta S_M)_{max}$ does not show monotonous change from $Er_{12}Co_7$ to $Ho_{12}Co_7$, and $Er_2Ho_{10}Co_7$ compound shows the minimum value of $(\Delta S_M)_{max}$.

Another important parameter to evaluate the magnetocaloric materials is refrigerant capacity (RC). RC can be calculated by the equation $RC = \int_{T_L}^{T_H} |\Delta S_M| dT$, where T_L and T_H are the temperatures corresponding to the both sides of half $(\Delta S_M)_{max}$, respectively [46]. The value of T_H-T_L is the full width at half maximum value of ΔS_M-T curve (δT_{FWHM}), which means the applicable temperature range of the MCE materials. All of the parameters, $(\Delta S_M)_{max}$, RC and δT_{FWHM}, are listed in Table 1. Since only one peak is observed in the ΔS_M-T curves of $Er_{12}Co_7$ compound, the value of δT_{FWHM} is somehow lower compared to those of the other $Er_{12-x}Ho_xCo_7$ compounds. The values of δT_{FWHM} of $Er_{12}Co_7$ compound for the field changes of 0–2 T and 0–5 T are 14.5 K and 22.8 K, respectively. According to the analysis of transition temperatures, T_t changes slightly and T_C increases rapidly as the content of Ho increases. The value of δT_{FWHM} for each compound is closely related to the interval of the transition temperatures. Therefore, δT_{FWHM} increases monotonously with increasing Ho content. The RC shows a similar trend to that of δT_{FWHM}, but $Er_2Ho_{10}Co_7$ compound is an exception because of its minimum value of $(\Delta S_M)_{max}$ among the $Er_{12-x}Ho_xCo_7$ compounds.

For practical applications of MCE materials in refrigerators, the materials with table-like ΔS_M-T curves are more important [27] because this type of MCE materials can achieve a much wider temperature range of refrigeration. Therefore, great efforts have been made to design and obtain MCE materials with plateau feature by mixing different materials, such as REFeSi (RE = Tb, Dy) [29]. Considering that each $Er_{12-x}Ho_xCo_7$ (x = 0, 4, 6, 8, 10, 12) compound shows good performance on MCE at different temperature zones, table-like ΔS_M-T curve can be realized by mixing and optimizing the $Er_{12-x}Ho_xCo_7$ compounds with different concentrations. Attempts have been tried for this composite compound, for example, $Ho_{12}Co_7$ and $Er_6Ho_6Co_7$ compounds are combined with the weight ratio of 58:42 to exhibit plateau feature and good MCE performance. The ΔS_M-T curves of $Ho_{12}Co_7$, $Er_6Ho_6Co_7$ and the mixed compound are shown in Fig 4(c). Under a field change of 0–5 T, the maximum value of ΔS_M for the newly obtained material is 16.7 J/kgK, and δT_{FWHM} and RC reach 38 K and 553 J/kg, respectively. The value of RC is comparable to $Ho_{12}Co_7$ compound and the δT_{FWHM} is larger than $Ho_{12}Co_7$ compound. Furthermore, there is a plateau in the ΔS_M-T curve, indicating that the mixed compounds of $Ho_{12}Co_7$ and $Er_6Ho_6Co_7$ with a weight ratio of 58:42 is more valuable for its potential applications for low-temperature refrigeration around 20–30 K.

4. Conclusions

The large MCE was found in polycrystalline $Er_{12}Co_7$ compound, which shows two transitions from AFM to FM and from FM to PM with increasing temperature. The maximum value of ΔS_M is 10.2 J/kgK under a field change of 0–2 T. Ho-substitution shows a great influence on the magnetic properties and MCE of $Er_{12}Co_7$ compound. The $Er_{12-x}Ho_xCo_7$ compounds were mixed to further tune their MCE properties. The mixed $Ho_{12}Co_7$ and $Er_6Ho_6Co_7$ compound with the optimized weight ratio of 58:42 exhibits plateau-type ΔS_M-T curve and excellent MCE performance, indicating its potential applications at low temperature.

Acknowledgements

This work was supported by the National Basic Research Program of China (973 Program No. 2014CB643700), the National Natural Science Foundation of China (Nos. 11274357, 51431009, 51501005 and 11504019) and the Fundamental Research Funds for the Central Universities (Nos. FRF-TP-15-010A1 and FRF-TP-15-005A1).

References

[1] V.K. Pecharsky, K.A. Gschneidner Jr., Magnetocaloric effect and magnetic refrigeration, J. Magn. Magn. Mater. 200 (1999) 44–56.
[2] K.A. Gschneidner Jr., V.K. Pecharsky, Magnetocaloric materials, Annu. Rev. Matter. Sci. 30 (2000) 387–429.
[3] J. Glanz, Making a bigger chill with magnets, Science 279 (1998), 2045–2045.
[4] O. Tegus, E. Brück, K.H.J. Buschow, F.R. de Boer, Transition-metal-based magnetic refrigerants for room-temperature applications, Nature 415 (2002) 150–152.
[5] V.K. Pecharsky, K.A. Gschneidner, Giant magnetocaloric effect in $Gd_5(Si_2Ge_2)$, Phys. Rev. Lett. 78 (1997) 4494–4497.
[6] F.X. Hu, B.G. Shen, J.R. Sun, Z.H. Cheng, G.H. Rao, X.X. Zhang, Influence of negative lattice expansion and metamagnetic transition on magnetic entropy change in the compound $LaFe_{11.4}Si_{1.6}$, Appl. Phys. Lett. 78 (2001) 3675–3677.
[7] H. Wada, Y. Tanabe, Giant magnetocaloric effect of $MnAs_{1-x}Sb_x$, Appl. Phys. Lett. 79 (2001) 3302–3304.
[8] F.X. Hu, B.G. Shen, J.R. Sun, G.H. Wu, Large magnetic entropy change in a heusler alloy $Ni_{52.6}Mn_{23.1}Ga_{24.3}$ single crystal, Phys. Rev. B 64 (2001) 132412.
[9] J. Liu, T. Gottschall, K.P. Skokov, J.D. Moore, O. Gutfleisch, Giant magnetocaloric effect driven by structural transition, Nat. Mater. 11 (2012) 620–626.
[10] F.W. Wang, X.X. Zhang, F.X. Hu, Large magnetic entropy change in $TbAl_2$ and $(Tb_{0.4}Gd_{0.6})Al_2$, Appl. Phys. Lett. 77 (2000) 1360–1362.
[11] X.X. Zhang, G.H. Wen, F.W. Wang, W.H. Wang, C.H. Yu, G.H. Wu, Magnetic entropy change in Fe-based compound $LaFe_{10.6}Si_{2.4}$, Appl. Phys. Lett. 77 (2000) 3072–3074.
[12] F.X. Hu, B.G. Shen, J.R. Sun, X.X. Zhang, Great magnetic entropy change in $La(Fe, M)_{13}$ (M=Si, Al) with Co doping, Chin. Phys. 09 (2000) 0550–0553.
[13] X.X. Zhang, F.W. Wang, G.H. Wen, Magnetic entropy change in RCoAl (R = Gd, Tb, Dy, and Ho) compounds candidate materials for providing magnetic refrigeration in the temperature range 10 K to 100 K, J. Phys. Condens. Matter 13 (2001) L747–L752.
[14] J. Liu, J.D. Moore, K.P. Skokov, M. Krautz, K. Lowe, A. Barcza, M. Katter, O. Gutfleisch, Exploring $La(Fe,Si)_{13}$-based magnetic refrigerants towards application, Scr. Mater. 67 (2012) 584–589.
[15] J. Lyubina, U. Hannemann, L.F. Cohen, M.P. Ryan, Novel $La(Fe,Si)_{13}$/Cu

composites for magnetic cooling, Adv. Energy Mater. 2 (2012) 1323–1327.
[16] G. Porcari, S. Fabbrici, C. Pernechele, F. Albertini, M. Buzzi, A. Paoluzi, J. Kamarad, Z. Arnold, M. Solzi, Reverse magnetostructural transformation and adiabatic temperature change in Co- and In-substituted Ni-Mn-Ga alloys, Phys. Rev. B 85 (2012) 024414.
[17] Y.Y. Gong, D.H. Wang, Q.Q. Cao, E.K. Liu, J. Liu, Y.W. Du, Electric field control of the magnetocaloric effect, Adv. Mater. 27 (2015) 801–805.
[18] L. Cui, L.C. Wang, Q.Y. Dong, F.H. Liu, Z.J. Mo, Y. Zhang, E. Niu, Z.Y. Xu, F.X. Hu, J.R. Sun, B.G. Shen, Effect of Cu doping on the magnetic and magnetocaloric properties in the HoNiAl intermetallic compound, J. Alloys Compd. 622 (2015) 24–28.
[19] H. Zhang, Y. Li, E. Liu, Y. Ke, J. Jin, Y. Long, B. Shen, Giant rotating magnetocaloric effect induced by highly texturing in polycrystalline DyNiSi compound, Sci. Rep. 5 (2015) 11929.
[20] Y. Zhang, B. Yang, G. Wilde, Magnetic properties and magnetocaloric effect in ternary REAgAl (RE=Er and Ho) intermetallic compounds, J. Alloys Compd. 619 (2015) 12–15.
[21] L. Li, D. Huo, H. Igawa, K. Nishimura, Large magnetocaloric effect in $TbCo_3B_2$ compound, J. Alloys Compd. 509 (2011) 1796–1799.
[22] S.B. Gupta, K.G. Suresh, Giant low field magnetocaloric effect in soft ferromagnetic ErRuSi, Appl. Phys. Lett. 102 (2013) 022408.
[23] L.C. Wang, Q.Y. Dong, J. Lu, X.P. Shao, Z.J. Mo, Z.Y. Xu, J.R. Sun, F.X. Hu, B.G. Shen, Low-temperature large magnetocaloric effect in the antiferromagnetic CeSi compound, J. Alloys Compd. 587 (2014) 10–13.
[24] J. Chen, B.G. Shen, Q.Y. Dong, F.X. Hu, J.R. Sun, Large reversible magnetocaloric effect caused by two successive magnetic transitions in ErGa compound, Appl. Phys. Lett. 95 (2009) 132504.
[25] L. Li, Y. Yuan, Y. Zhang, R. Pöttgen, S. Zhou, Magnetic phase transitions and large magnetic entropy change with a wide temperature span in HoZn, J. Alloys Compd. 643 (2015) 147–151.
[26] X.Q. Zheng, J. Chen, Z.Y. Xu, Z.J. Mo, F.X. Hu, J.R. Sun, B.G. Shen, Nearly constant magnetic entropy change and adiabatic temperature change in PrGa compound, J. Appl. Phys. 115 (2014), 17A938.
[27] X.Q. Zheng, H. Wu, J. Chen, B. Zhang, Y.Q. Li, F.X. Hu, J.R. Sun, Q.Z. Huang, B.G. Shen, The physical mechanism of magnetic field controlled magnetocaloric effect and magnetoresistance in bulk PrGa compound, Sci. Rep. 5 (2015) 14970.
[28] L. Li, O. Niehaus, M. Johnscher, R. Pöttgen, Magnetic properties and tuneable magnetocaloric effect with large temperature span in $GdCd_{1-x}Ru_x$ solid solutions, Intermetallics 60 (2015) 9–12.
[29] H. Zhang, Y.J. Sun, E. Niu, L.H. Yang, J. Shen, F.X. Hu, J.R. Sun, B.G. Shen, Large magnetocaloric effects of RFeSi (R=Tb and Dy) compounds for magnetic refrigeration in nitrogen and natural gas liquefaction, Appl. Phys. Lett. 103 (2013) 202412.
[30] L. Li, K. Nishimura, G. Usui, D. Huo, Z. Qian, Study of the magnetic properties and magnetocaloric effect in RCo_2B_2 (R=Tb, Dy and Ho) compounds, Intermetallics 23 (2012) 101–105.
[31] L. Li, K. Nishimura, D. Huo, Z. Qian, T. Namiki, Critical behaviour of the RCo_3B_2 (R=Gd, Tb and Dy) compounds, J. Alloys Compd. 572 (2013) 205–208.
[32] Z.J. Mo, J. Shen, L.Q. Yan, C.C. Tang, L.C. Wang, J.F. Wu, J.R. Sun, B.G. Shen, Magnetic property and magnetocaloric effect in TmCoAl compound, Intermetallics 56 (2015) 75–78.
[33] W. Adams, J.M. Moreau, E. Parthe, J. Schweizer, $R_{12}Co_7$ compounds with R = Gd, Tb, Dy, Ho, Er, Acta Cryst. B32 (1976) 2697–2699.
[34] J.Q. Deng, Y.H. Zhuang, J.Q. Li, J.L. Huang, Magnetic properties of $Tb_{12}Co_7$, Phys. B 391 (2007) 331–334.
[35] X. Chen, Y.H. Zhuang, Magnetocaloric effect of $Gd_{12}Co_7$, Solid State Commun. 148 (2008) 322–325.
[36] Q.Y. Dong, J. Chen, X.Q. Zhang, X.Q. Zheng, J.R. Sun, B.G. Shen, Magnetic phase transition and magnetocaloric effect in $Dy_{12}Co_7$ compound, J. Appl. Phys. 114 (2013) 173911.
[37] Z.G. Zheng, X.C. Zhong, H.Y. Yu, Z.W. Liu, D.C. Zeng, Magnetic phase transitions and magnetocaloric properties of $(Gd_{12-x}Tb_x)Co_7$ alloys, J. Appl. Phys. 109 (2011), 07A919.
[38] X.Q. Zheng, X.P. Shao, J. Chen, Z.Y. Xu, F.X. Hu, J.R. Sun, B.G. Shen, Giant magnetocaloric effect in $Ho_{12}Co_7$ compound, Appl. Phys. Lett. 102 (2013) 022421.
[39] D. Gignoux, J.C. Gomez-Sal, D. Paccard, Magnetic properties of a Tb_3Ni single crystal, Solid State Commun. 44 (1982) 695–700.
[40] S.K. Banerjee, On a generalised approach to first and second order magnetic transitions, Phys. Lett. 12 (1964) 16–17.
[41] A. Fujita, Y. Akamatsu, K. Fukamichi, Itinerant electron metamagnetic transition in $La(Fe_xSi_{1-x})_{13}$, J. Appl. Phys. 85 (1999) 4756–4758.
[42] D. Gignoux, D. Schmitt, Rare earth intermetallics, J. Magn. Magn. Mater. 100 (1991) 99–125.
[43] M. Khan, K.A. Gschneidner, V.K. Pecharsky, The effect of Er doping on the spin reorientation transition in $Ho_{1-x}Er_xAl_2$, J. Magn. Magn. Mater. 324 (2012) 1381–1384.
[44] T. Samanta, I. Das, S. Banerjee, Giant magnetocaloric effect in antiferromagnetic $ErRu_2Si_2$ compound, Appl. Phys. Lett. 91 (2007) 152506.
[45] H. Oesterreicher, F.T. Parker, Magnetic cooling near Curie temperatures above 300 K, J. Appl. Phys. 55 (1984) 4334–4338.
[46] K.A. Gschneidner Jr., V.K. Pecharsky, A.O. Pecharsky, C.B. Zimm, Recent developments in magnetic refrigeration, Mater. Sci. Forum 315–317 (1999) 69–76.